A R T I C L E

Saliva as a noninvasive sampling matrix for therapeutic drug monitoring of intravenous busulfan in Chinese patients undergoing hematopoietic stem cell transplantation: A prospective population pharmacokinetic and simulation study

Baohua Xu[1,2] | **Ting Yang**[3] | **Jianxing Zhou**[1,2] 🞔 | **You Zheng**[1,2] | **Jingting Wang**[4] |
Qingxia Liu[1,2] 🞔 | **Dandan Li**[1,2] | **Yifan Zhang**[5] | **Maobai Liu**[1] | **Xuemei Wu**[1] 🞔

[1]Department of Pharmacy, Fujian Medical University Union Hospital, Fuzhou, Fujian, China

[2]School of Pharmacy, Fujian Medical University, Fuzhou, Fujian, China

[3]Department of Hematology, Fujian Medical University Union Hospital, Fuzhou, Fujian, China

[4]College of Pharmacy, University of Michigan, Ann Arbor, Michigan, USA

[5]Shanghai Institute of Materia Medica, Chinese Academy of Sciences, Shanghai, China

Correspondence
Maobai Liu and Xuemei Wu, Department of Pharmacy, Fujian Medical University Union Hospital, 29 Xinquan Rd., Gulou District, Fuzhou 350001, Fujian, China.
Email: liumb0591@fjmu.edu.cn; wuxuemei@fjmu.edu.cn

Abstract

Therapeutic drug monitoring (TDM) of busulfan (BU) is currently performed by plasma sampling in patients undergoing hematopoietic stem cell transplantation (HSCT). Saliva samples are considered a noninvasive TDM matrix. Currently, no salivary population pharmacokinetics (PopPKs) model for BU available. This study aimed to develop a PopPK model that can describe the relationship between plasma and saliva kinetics in patients receiving intravenous BU. The performance of the model in predicting the area under the concentration-time curve at steady state (AUC_{ss}) based on saliva samples is evaluated. Sixty-six patients with HSCT were recruited and administered 0.8 mg/kg BU intravenously. A PopPK model for saliva and plasma was developed using the nonlinear mixed effects model. Bayesian maximum a posteriori (MAP) optimization was used to estimate the model's predictive performance. Plasma and saliva PKs were adequately described with a one-compartment model and a scaled central compartment. Body surface area correlated positively with both clearance and apparent volume of distribution (Vd), whereas alkaline phosphatase correlated negatively with Vd. Simulations demonstrated that the percentage root mean squared prediction error and lower and upper limits of agreements reduced to 10.02% and −16.96% to 22.86% based on five saliva samples. Saliva can be used as an alternative matrix to plasma in TDM of BU. The AUC_{ss} can be predicted from saliva concentration by Bayesian MAP optimization, which can be used to design personalized dosing for BU.

Baohua Xu and Ting Yang has contributed equally to this article.

[Correction added on 02 Aug 2023, after first online publication: "Baohua Xu and Ting Yang has contributed equally to this article." has been updated in this version.]

Study Highlights

WHAT IS THE CURRENT KNOWLEDGE ON THE TOPIC?

Busulfan (BU) has a narrow therapeutic range and high intra- and interpatient variability. The conventional therapeutic drug monitoring (TDM) sampling matrix is plasma. There is no population pharmacokinetic (PopPK) model with saliva as a TDM matrix for the intravenous BU.

WHAT QUESTION DID THIS STUDY ADDRESS?

Traditional TDM necessitates multiple blood draws, which may contribute to infection or anemia in special populations. With the advantages of a noninvasive, quick, and easy sampling approach, saliva was assessed as an alternative matrix for BU TDM.

WHAT DOES THIS STUDY ADD TO OUR KNOWLEDGE?

A detailed description of BU PK in saliva and plasma of the Chinese population, which is strongly influenced by body surface area and alkaline phosphatase. The area under the concentration-time curve at steady state of BU can be predicted from saliva concentration by Bayesian maximum a posteriori optimization and yields acceptable prediction errors.

HOW MIGHT THIS CHANGE DRUG DISCOVERY, DEVELOPMENT, AND/OR THERAPEUTICS?

The saliva PopPK model was developed by nonlinear PK modeling techniques, which can be potentially used to optimize the dosing regimen of BU in the clinic.

INTRODUCTION

Hematopoietic stem cell transplantation (HSCT) has become the preferred treatment for hematologic malignancies in children and adults.[1] Patients must receive a course of high-dose chemotherapy or chemotherapy combined with high-dose radiotherapy before HSCT. The treatment is called a conditioning regimen, one of the critical links of HSCT and an essential determinant of successful transplantation. Cyclophosphamide combined with total body irradiation or busulfan (BU) are the two most common conditioning regimens.[2,3]

BU is a bifunctional alkylating agent. After entering the human body, it is hydrolyzed to release methane sulfonic acid groups, which generate an activated carbon ion and alkylates with guanine in DNA, thus destroying the structure and function of DNA.[4] BU can be administered orally and intravenously. The oral formulation of BU is characterized by rapid absorption with highly variable bioavailability ranging from 70% to 90% and hepatic first-pass effects.[5] Besides, it has been estimated that the inter-patient variability associated with oral BU was up to 10-fold or more.[6] These problems significantly interfere with the reproducibility and reliability of pharmacokinetic (PK) information.[7] The intravenous (i.v.) infusion of 0.8 mg/kg is as effective as the oral administration of 1 mg/kg.[8] Forty to 60% of patients can reach the target treatment range of exposure, which is expressed as the area under the concentration-time curve (AUC).[9] Because i.v. BU could significantly decrease the incidence of hemostatic derangements and hepatic venular occlusive disease,[10] it is preferable in the clinic. One-compartment model with a terminal half-life of 2–3 h can adequately describe the PKs of BU.[11]

BU has a narrow therapeutic range in which efficacy and adverse drug reactions (ADRs) are closely related to AUC or steady-state plasma concentration.[12] Generally, patients receive i.v. BU (0.8 mg/kg) every 6 h as a 2-h infusion. The European Medicines Agency (EMA) recommends that the AUC at each dose should be between 900 and 1500 μmol*min/L, and the US Food and Drug Administration (FDA) recommended range is 900–1350 μmol*min/L.[12,13] AUC lower than 900 μmol*min/L may contribute to migration failure,[14] whereas AUC higher than 1500 μmol*min/L can lead to a higher incidence of venular occlusive disease.[15] Although individualized dosing is based on body surface area (BSA) or body weight, nearly half of the patients cannot reach the target treatment range under the regimen.[16] Therefore, therapeutic drug monitoring (TDM) is necessary to improve efficacy, reduce the incidence of ADR, and ensure adequate dosing regimens.

The conventional TDM sampling matrix is plasma. It is painful and invasive and may contribute to infection or anemia in special populations,[17,18] thus further limiting the number of sample collections. Saliva is a noninvasive TDM matrix with the advantages of readily available and increased sampling frequency. The sampling personnel does not require professional training. Moreover, there are

no contraindications for saliva collection except for inflammations or pathological changes of oro-mucosal.[19] The previous study has shown that it is feasible to use saliva as the matrix of TDM for orally given BU, and the correlation between BU salivary and plasma concentrations are sufficiently good.[20] Furthermore, TDM generally requires sampling at multiple time points. Compared with the traditional sampling method, the population pharmacokinetic (PopPK) model can reduce the number of samples and be more convenient. Many studies have established the PopPK model of BU in patients with HSCT.[21–23] There is no PopPK model with saliva as a TDM matrix for the i.v. BU.

This study aimed to develop a PopPK of i.v. BU can describe the relationship between plasma and salivary BU concentrations. The performance of the PopPK model to predict AUC at steady state (AUC_{ss}) based on saliva samples was evaluated.

METHODS

Subjects

A total of 66 patients (54 adults and 12 children) who had hematologic malignances and received allogeneic HSCT were enrolled in Fujian Medical University Union Hospital from November 2020 to November 2021. The study was approved by an Independent Ethical Committee at Fujian Medical University Union Hospital. The approval number is 2019KJCX024 and the approved date is November 28, 2019. Informed consent was obtained prior to study-mandated procedures.

Study design

All patients received a pretreatment regimen based on i.v. BU before transplantation. Four different conditioning regimens which consisted of BU in combination with (1) cytarabine + fludarabine + cyclophosphamide, (2) cytarabine + cyclophosphamide, (3) cytarabine + fludarabine, and (4) fludarabine were used for bone marrow ablation. Patients received i.v. BU every 6 h as a 2-h infusion for 4 consecutive days. The dosage of BU was 0.8 mg/kg, which was calculated using adjusted ideal body weight (AIBW).[24]

Sample collection and bio-analytical assay

Paired blood samples and saliva samples were collected just before (0h) and at 0.5, 2, 2.5, 3, 4, and 6 h after the beginning of the first dose. Venous blood (2.0 mL) was collected using the EDTA anticoagulation tubes. Saliva samples were collected using a Salivette device (SARSTEDT, Numbrecht, Germany). The subjects were instructed to chew the cotton swab for 30–60 s, then put the cotton swab back into the saliva collection tube. Plasma and saliva samples obtained by centrifugation were assayed by a validated high-performance liquid chromatography–tandem mass spectrometry assay technique.[25] The calibration standards had a linear relationship with plasma and saliva concentrations ranging from 0.05 to 2.5 μg/mL. The lower limit of detection was 3 ng/mL, at which the signal level of BU reached at least three times the signal noise of the baseline.

Statistical and correlation analysis

Descriptive statistics were performed in SPSS Statistics version 20.0 (IBM Corp). The plasma and saliva concentrations at different time points were fitted by linear regression. Pearson correlation analysis was used to investigate their correlation. It is considered that the difference is statistically significant when $p < 0.05$.

Population pharmacokinetic analysis

PopPK analysis was carried out by nonlinear mixed effect modeling, using the First Order Conditional Estimation with interaction within the NONMEM version 7.5.0 (ICON Development Solutions). Pirana version 2.9.7 (Certara) was used as the modeling interface. Data handling and visualization were performed in R version 4.1.3 (R Foundation for Statistical Computing), RStudio version 1.2.5001 (RStudio), and GraphPad Prism version 8.0.0 (GraphPad Software).

A stepwise modeling approach developed an integrated PopPK model describing BU in saliva and plasma. First, the basic PopPK model of BU in plasma adopted a one-compartment structure model with a constant rate infusion[24,26] using ADVAN1 TRANS2 subroutine in NONMEM. Interindividual variability (IIV) was estimated on all structural parameters of the investigated plasma model. Different error models (additive, proportional, or additive-proportional) were tested to account for residual variability. After identifying a suitable model for plasma BU concentration, saliva measurements were added to the model by testing either a separate saliva compartment or a "scale" parameter assigned to the plasma compartment.[27] Separate error models accounted for residual variability of the BU concentrations in saliva.

IIV on the structural PK parameters was modeled using an exponential error model as follows:

$$P_i = \theta_P \times e^{\eta_i} \tag{1}$$

P_i represents the estimated ith P for the ith individual calculated from the typical population value θ_P, and η_i is independent, identically distributed random variables with mean 0 and variance ω.[2] Residual IIV was estimated by a proportional or additive, or combined error model:

$$Y_{ij,obs} = Y_{ij,p} \times \left(1 + \varepsilon_{ij,p}\right) + \varepsilon_{ij,a} \tag{2}$$

Y_{ij}, obs represents the ith measured concentration in the jth individual, $Y_{ij,p}$ represents the ith predicted concentration for the jth individual, $\varepsilon_{ij,p}$ represents ith proportional error for the jth individual, $\varepsilon_{ij,a}$ represents ith additive error for the jth individual.

Patient-specific factors considered for covariate testing included sex, age, height (HT), weight (WT), body mass index (BMI), ideal body weight (IBW), AIBW, BSA, total bilirubin, serum albumin, alanine transaminase (ALT), aspartate transaminase, gamma-glutamyl transferase, alkaline phosphatase (ALP), lactic dehydrogenase, creatinine, creatinine clearance (CLCR), and concomitant drugs (fludarabine, cyclosporine, phenytoin sodium, palonosetron). Individual covariates were initially screened based on the scatter plots of covariates versus individual parameters. The potential covariates analysis was further performed using a stepwise procedure based on the changes in objective function value (OFV). During forward inclusion, the significance level was set to 0.05 (df = 1, ΔOFV = 3.84). During backward elimination, the significance level was set to 0.001 (df = 1, ΔOFV = 10.83). As body size is the commonly used parameter to calculate BU dosing in clinical practice, the influence of each of the body size parameters in BU PK was evaluated using univariate NONMEM analyses. Then the best "body size index model" was selected to screen the influence of the other covariates.[24] Continuous covariates were included in the model as a power equation function:

$$P = \theta_P \times \left(\frac{COV}{COV\_median}\right)^{\theta_{cov}} \tag{3}$$

where P is an individual value for a PK parameter, θ_P is the typical parameter, θcov represents the magnitude of the covariate effect, COV is a covariate type, and COV_median is the median value of the covariate.

The categorical covariates were assigned values of 0 and 1 and were coded in NONMEM as a proportional equation function:

$$P = \theta_P \times \left(1 + \theta_{cov} \times COV\right) \tag{4}$$

Goodness-of-fit (GOF) plots, η-shrinkage, ε-shrinkage, and residual standard error (RSE) were used for model evaluation. The GOFs included the scatter plots of observation concentrations versus individual predicted concentrations (IPRED) and population predicted concentrations (PRED), conditional weighted residuals (CWRES) versus PRED and time after dose. Bootstrap analyses ($n = 1000$) were used to assess the model's robustness. Visual predictive check (VPC) was used to validate the final model performance.[28]

Simulations and evaluation of the predictability of the model

A simulation cohort ($n = 3000$) with a positive skew distribution of BSA and corresponding normal distribution of ALP was prepared. PK profile after administration of 0.8 mg/kg for 16 times (q6h) was simulated for each subject, taking into account IIV and residual variability. Simulated saliva and plasma samples were obtained at 2, 3, 4, 5, and 6 h after the first dose. AUC_{ss} within each dose interval was used to examine the model predictability, which is equal to the AUC from zero to infinity ($AUC_{0-\infty}$) after dose one. Simulated AUC_{ss} in plasma was calculated for each subject based on the simulated clearance (CL) ($AUC_{ss} = DOSE/CL$). Predicted AUC_{ss} in plasma was obtained using traditional linear regression or Bayesian maximum a posteriori (MAP) optimization[29,30] and zero to five simulated saliva samples.

$AUC_{0-\infty}$ was calculated according to the actual BU concentration in plasma and saliva using the linear trapezoidal rule by summing the areas from zero to the time of last measured concentration and the extrapolated area. The slope (λz) of the terminal phase of the BU concentration-time profile was calculated by least squares minimization. The extrapolated area was obtained by dividing the last observed BU concentration by λz. The relationship between $AUC_{0-\infty,plasma}$ and $AUC_{0-\infty,saliva}$ was calculated using the linear regression formula. A multiple linear regression analysis was used to evaluate the $AUC_{0-\infty,saliva}$ and saliva concentrations (peak and trough concentrations). Based on the simulated saliva samples obtained at 2 and 6 h after the first dose, the derived equations were used to predict the corresponding $AUC_{0-\infty,plasma}$.

The simulated AUC_{ss} was compared with the predicted AUC_{ss} to indicate the predictability of the model.[31] The percentage root mean square prediction error (RMSPE%) was used to quantify the predictive performance of each sampling scenario.[32] In addition, the average bias and limits of agreement (LOA) of the predictions were calculated according to the methods of Bland and Altman,[33] expressed as percentages.

RESULTS

Demographic characteristics and correlation analysis

Table 1 depicts the demographic characteristics of the included patients. Of the 406 pairs of plasma and saliva samples, 387 saliva samples provided enough volume for the analysis. Nineteen (4.68%) saliva samples were below the lower limit of quantitation, which were deleted according to M1 method.[34] The observed plasma $AUC_{0-\infty}$ of 36 patients (54.5%) were within the target range of 900–1500 μmol*min/L after the first dose. The BU peak in both matrices appeared at 2h after administration. BU concentrations in plasma and saliva were different (1.16 ± 0.29 μg/mL vs. 0.99 ± 0.27 μg/mL, $p < 0.01$). Table 2 depicts the saliva/plasma ratio (S/P ratio) and correlation coefficient of the BU saliva and plasma concentration at each time-point. A good correlation between saliva and plasma BU concentrations was observed ($R = 0.80$, $p < 0.01$), and the S/P ratio was 0.89 ± 0.22. Pearson correlation coefficient between the saliva and plasma concentration at all time-points ranged from 0.45 to 0.92 ($p < 0.01$), indicating that the saliva concentration was positively correlated with the plasma concentration.

PopPK model

Considering both OFV and RSE, a proportional error model was selected for the plasma model. Saliva concentrations of BU were added to the plasma model. The use of a scale-factor to the plasma compartment was superior to a separate saliva compartment ($\Delta OFV = -82.52$).

TABLE 1 Demographics of patients.

Parameter	Value
Enrolled patients, n	66
Males, n (%)	46 (69.70)
Age (years), median (range)	42 (6–63)
Height (cm), median (range)	160 (123–190)
Weight (kg), median (range)	60.70 (25~90)
BSA (m^2), median (range)	1.69 (0.92–2.14)
ALP (IU/L), median (range)	74 (36–253)
Total saliva samples, n	406
Analyzed, n	387
Failed, n	19
Total plasma samples, n	406
Analyzed, n	406
Failed, n	0

Abbreviations: BSA, body surface area; ALP, alkaline phosphatase.

TABLE 2 Correlation analysis ($\bar{x} \pm s$, μg/mL).

	0.5h	1.0h	1.5h	2.0h	2.5h	3h	4h	5h	6h
n	14	16	9	58	70	62	59	35	64
Plasma concentration	0.59 ± 0.15	0.71 ± 0.18	0.98 ± 0.29	1.16 ± 0.29	1.00 ± 0.26	0.89 ± 0.23	0.69 ± 0.18	0.58 ± 0.17	0.42 ± 0.14
Salivary concentration	0.53 ± 0.19	0.61 ± 0.16	0.88 ± 0.31	0.99 ± 0.27	0.91 ± 0.27	0.74 ± 0.21	0.60 ± 0.21	0.50 ± 0.18	0.37 ± 0.13
S/P ratio	0.90 ± 0.12	0.87 ± 0.14	0.88 ± 0.21	0.88 ± 0.22	0.92 ± 0.24	0.85 ± 0.19	0.89 ± 0.24	0.89 ± 0.32	0.90 ± 0.20
R	0.92	0.77	0.85	0.47	0.59	0.64	0.60	0.45	0.71
p value	<0.01	<0.01	<0.01	<0.01	<0.01	<0.01	<0.01	<0.01	<0.01

Abbreviation: S/P, saliva/plasma ratio.

A proportional error model was used for the saliva part of the model. The conceptual model for BU in plasma and saliva is depicted in Figure 1. The example data file and model code are shown in Table S1 and Table S2, respectively. The PK parameters of the structural model are shown in Table 3. All parameters were estimated with low RSE and shrinkage.

Individual covariates were initially screened by scatter plots of covariates versus individual parameters. These plots showed that ALT, ALP, CREA, CLCR, AGE, WT, HT, BMI, IBW, AIBW, and SEX might be the possible covariates affecting the apparent volume of distribution (Vd), whereas CL could be affected by ALP, CREA, CLCR, AGE, WT, HT, BMI, IBW, and AIBW. Stepwise forward inclusion of BSA as a power function covariate on Vd and CL led to the most significant decrease in OFV (ΔOFV $=-66.0$ and -29.0). ALP was included as a covariate on Vd as a power function (ΔOFV $=-38.1$). After backward elimination, these covariates were retained. None of the other tested covariates improved the model. The parameter estimates of the final model are presented in Table 3. The results indicated a positive correlation between BSA and CL or Vd, whereas ALP and Vd were negatively correlated.

GOF plots obtained from the final model for saliva are shown in Figure S1 (the GOF plots of final plasma model are shown in Figure S2). Compared to the structural model (Figure S3; the GOF plots of structural plasma model are shown in Figure S4), the scatter plot of observation concentrations versus IPRED and PRED indicated no structural bias and an improved fit of the final model. The CWRES of the final model showed a relatively even distribution around zero, and 95% were within an acceptable range (-2 to 2).

Bootstrap analysis ($n=1000$) was used to evaluate the robustness of the final model, in which 1000 runs were successful. The steady rate was 100%. The median and 95% confidence intervals (CIs) for the bootstrap parameter estimates are summarized in Table 3. The parameter estimates of the final model were similar to the median values of the bootstrap analysis and within the 95% CIs.
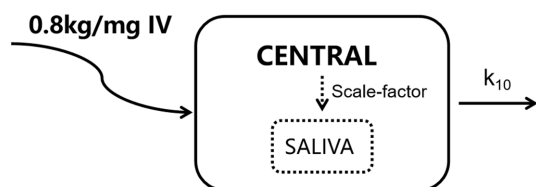

FIGURE 1 The conceptual model for BU PK in plasma and saliva. The solid lines: BU PK in plasma; the dashed lines: BU PK in saliva; k_{10}: the elimination rate from the central compartment; scale-factor: the scaling factor to describe BU concentrations in plasma assigned to the saliva compartment. BU, busulfan; PK, pharmacokinetic.

These results supported the reliability of the parameter estimates and indicated the stability of the final model.

The VPC plot (Figure 2; the VPC plot of final plasma model is shown in Figure S5) confirmed satisfactory predictive performance of the final model, as almost all the observed values were positioned within the 95% CIs of the 5th, 50th, and 95th percentiles.

Simulations

Predicted AUC$_{ss}$ in plasma using MAP without any simulated saliva sample leads to an RMSPE% of 23.08% and an average proportional bias of -0.13% (95% LOA -43.35% to 43.10%), indicating a high level of uncertainty in predicting individual AUC$_{ss}$. Under this scenario with one saliva sample, the RMSPE% and the average proportional bias were 13.74% and 4.26%, respectively. The LOA was reduced from -23.40% to 31.92%. The results suggested that the uncertainty of predicting individual AUC$_{ss}$ was significantly reduced by adding a saliva sample. There was a correlation between predicted and simulated AUC$_{ss}$ ($R=0.79$, $p<0.01$). In the case of five saliva samples, the RMSPE% was 10.02%, with an average proportional bias was 2.95%, and the LOA of -16.96% to 22.86% (Figure 3a). The results of predictions under the other scenarios are shown in Table 4. The RMSPE% gradually decreased, and the LOA gradually narrowed with increasing the number of saliva samples. The predicted and simulated AUC$_{ss}$ were correlated (Table 4) for all scenarios when Bayesian MAP optimization was applied.

The linear regression equation for the relationship between AUC$_{0-\infty,plasma}$ and AUC$_{0-\infty,saliva}$ was AUC$_{0-\infty,plasma}=$ AUC$_{0-\infty,saliva}\times 0.89+343.78$ ($R=0.63$, $p<0.01$). The estimated multiple linear regression equation was AUC$_{0-\infty,saliva}=385.23\times C_{peak}+2658.56\times C_{trough}-141.00$ ($R=0.97$, $p<0.01$). Compared to Bayesian MAP optimization, the predicted AUC based on linear regression led to a larger RMSPE% (15.29%), with a proportional bias of 0.75% (LOA -29.93% to 31.42%; Figure 3b). It indicated that the linear regression had higher uncertainty in predicting individual AUC$_{ss}$.

DISCUSSION

To the best of our knowledge, this is the first study to establish a PopPK model of i.v. BU based on saliva and plasma concentration in patients undergoing HSCT. In the final model, BSA was taken as the covariate of CL and Vd, and ALP as the covariate of Vd. The potential use of saliva concentration for prediction AUC$_{ss}$ was also assessed by Bayesian MAP optimization. The results showed that the

TABLE 3 Parameter estimates of the PopPK model and bootstrap results.

Parameter	Base model, OFV = −2192.96			Final model, OFV = −2304.20			Bootstrap results, ($n = 1000$)		
	Estimate	RSE (%)[k]	Shrinkage (%)	Estimate	RSE (%)	Shrinkage (%)	Estimate	2.5th%	97.5th%
θ_{CL} (L/h)[a]	7.89	4	–	8.24	3	–	8.24	7.75	8.77
θ_{Vd} (L)[b]	28.30	4	–	29.70	2	–	29.65	28.32	31.14
$\theta_{Scale-factor}$[c]	0.88	2	–	0.88	2	–	0.88	0.84	0.91
IIV_{CL} (%)[d]	28.20	8	2	22.00	8	4	21.53	17.93	24.79
IIV_{Vd} (%)[e]	27.50	12	4	13.60	18	14	13.02	8.10	17.90
ε_{plasma}(%)[f]	12.88	18	12	12.92	17	10	12.90	10.62	14.93
ε_{saliva}(%)[g]	22.52	22	3	22.50	22	3	22.09	17.87	28.13
θ_{BSA-CL}[h]	–	–	–	0.99	12	–	0.99	0.76	1.27
θ_{BSA-Vd}[i]	–	–	–	1.03	10	–	1.03	0.77	1.22
θ_{ALP-Vd}[j]	–	–	–	−0.20	26	–	−0.20	−0.31	−0.09

[a]The clearance of the central compartment.

[b]The apparent volume of distribution of the central compartment.

[c]Scaling factor to describe BU concentrations in saliva assigned to the saliva central compartment;

[d]IIV of CL.

[e]IIV of Vd.

[f]Residual intra-individual variability of CL.

[g]Residual intra-individual variability of Vd.

[h]Power equation exponent BSA on CL.

[i]Power equation exponent BSA on Vd.

[j]Power equation exponent ALP on Vd.

[k]Relative standard error.

$$CL = \theta_{CL} \times \left(\frac{BSA}{1.69} \right)^{\theta_{BSA\_CL}} \times e^{\eta}.$$

$$Vd = \theta_{Vd} \times \left(\frac{BSA}{1.69} \right)^{\theta_{BSA\_Vd}} \times \left(\frac{ALP}{74} \right)^{\theta_{ALP\_Vd}} e^{\eta}.$$

Abbreviations: ALP, alkaline phosphatase; BSA, body surface area; BU, busulfan; CL, clearance; IIV, interindividual variability; OFV, objective function value; PopPK, population pharmacokinetic; Vd, volume of distribution.

developed model could predict the AUC_{ss}, with an RMSPE% as low as 10.02% and a 95% proportional LOA of −16.96% to 22.86% under the scenario of using five saliva samples. Therefore, this PopPK model can be used for personalized dosing of BU based on noninvasive salivary sampling.

The volume of the saliva sample for analysis was further reduced to 50 μL compared with the study of Rauh et al.,[20] which is convenient for TDM in the pediatric population. The time to reach the maximum plasma concentration in both matrices occurred at the end of infusion, which was consistent with a study by Bezinelli et al.[35] Generally, the BU saliva concentrations were lower than plasma concentrations, with the S/P ratio close to 0.89. This result was different from the reports by Rauh et al.[20] (S/P ratio = 1.09) and Bezinelli et al.[35] (average S/P = 1.00), but in line with the observation of de Paula Eduardo et al.[36] (average S/P ratio = 0.92). The composition of plasma and saliva, most notably proteins, may explain the difference. A lower amount of protein was reported in saliva than in plasma.[20] Another reason associated with the discrepancy in the S/P ratio may be related to the patient's age and route of administration. BU was administered intravenously in our study, whereas it was given orally in the study of Rauh et al.[20] Bezinelli et al.[35] that only enrolled adult patients in their study, whereas we included both adult and pediatric patients. Children showed a higher clearance than adults due to faster metabolization and rapid drug distribution.[37]

The saliva concentrations showed excellent correlation with plasma concentrations at 0.5 to 1.5 h ($R = 0.77 \sim 0.92$) after dosing, whereas it showed moderate correlation at 2 to 6 h ($R = 0.45 \sim 0.71$). In the current study, BU was usually given at 8:00–10:00 in the morning. Patients started their lunch at 11:30–13:00. Food can stimulate the secretion of saliva, accelerate the flow rate of saliva, and eventually dilute saliva BU concentration.[38,39] In addition, intraoral food residue might play a role in the lower correlation between the two metrics due to the elevated sound during analysis.

FIGURE 2 Visual predictive check of the saliva model ($n = 1000$). Black circles: observed BU concentrations in the saliva; red line: the 50th percentiles of the observed concentrations; blue lines: the 5th and 95th percentiles of the observed concentrations; red shadow: 95% confidence interval of the median prediction; blue shadow: 95% confidence intervals of the 5th and 95th percentiles of the predictions. BU, busulfan.
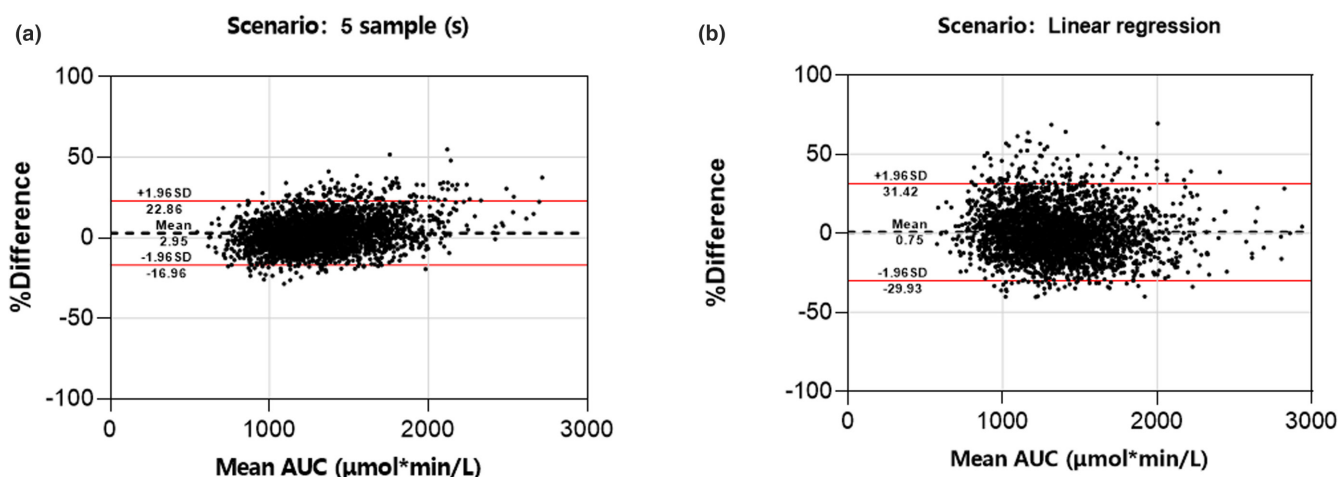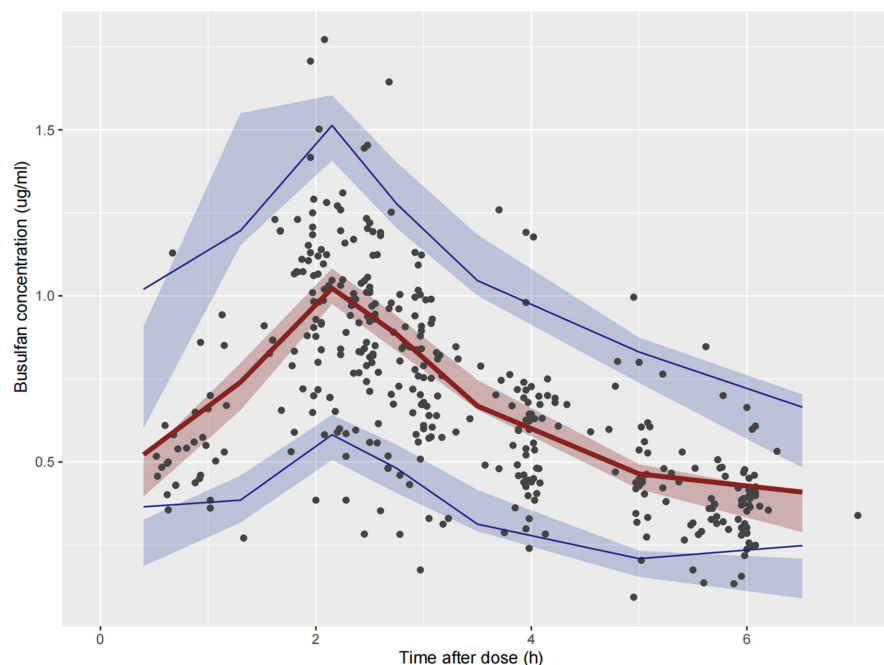

FIGURE 3 Visualization of the predictive capability of (a) Bayesian MAP optimization (based on 5 saliva samples) and (b) linear regression (based on 2 saliva samples). The dotted line and red lines display the proportional bias and the lower and upper limits of agreement of predicted AUC$_{ss}$, respectively. The x-axis: the mean of the predicted and simulated AUC$_{ss}$; the y-axis: the proportional difference between the predicted and simulated AUC$_{ss}$. For the proportional bias plots of other scenarios, please refer to Figure S8. AUC$_{ss}$, area under the concentration-time curve at steady state; MAP, maximum a posteriori.

Several investigators have demonstrated the feasibility and accuracy of saliva TDM in artemisinin, digoxin, and many other drugs.[40–43] Most studies focused on the linear correlation between saliva and plasma drug concentration. This study further incorporated saliva concentration into the nonlinear mixed effects model, taking into account the impact of intra-individual and IIV on PK simultaneously. A one-compartment model with a scale-factor of 0.88 can adequately describe the PKs of BU in plasma and saliva. The identified scale-factor can describe BU distribution from plasma to saliva. We also tested another structural model, and saliva measurements were assigned to a separate,

kinetically different compartment (Figure S6). It is similar to a hypothetical effect compartment. The first-order transport rate from the plasma compartment to the saliva compartment was expressed as k_{12}, whereas the first-order rate of BU elimination from the saliva compartment was expressed as k_{20}. For the structural model, a CL of 6.22 L/h, a k_{12} of 0.074 h^{-1}, and k_{20} of 10 h^{-1} were estimated. Given the unacceptable RSE% of k_{20} (87%) and the higher OFV, the one-compartment model with a scaled central saliva compartment was selected as the final model.

Body size (e.g., AIBW, BW, or BSA) had been identified as a covariate for Vd and CL in previous BU PopPK

TABLE 4 The simulation used different saliva samples to determine the predictive capability of AUC

	RMSPE%[a]	Bias (%)	LLOA (%)[b]	ULOA (%)[c]	R
No sample, Population model	23.08	−0.13	−43.35	43.10	0.31 ($p < 0.01$)
Two samples, Linear regression	15.29	0.75	−29.93	31.42	0.79 ($p < 0.01$)
One sample, Bayesian[d]	13.74	4.26	−23.40	31.92	0.79 ($p < 0.01$)
Two samples, Bayesian[e]	13.45	4.41	−22.63	31.44	0.80 ($p < 0.01$)
Three samples, Bayesian[f]	12.06	3.71	−20.43	27.86	0.84 ($p < 0.01$)
Four samples, Bayesian[g]	11.55	3.59	−19.50	26.67	0.85 ($p < 0.01$)
Five samples, Bayesian[h]	10.02	2.95	−16.96	22.86	0.89 ($p < 0.01$)

[a]Percentage root mean squared prediction error.

[b]LLOA (−1.96 SD).

[c]ULOA (+1.96 SD).

[d]One sample: sample at 6 h postdose.

[e]Two samples: samples at 2 and 6 h postdose.

[f]Three samples: samples at 2, 4, and 6 h postdose.

[g]Four samples: samples at 2, 3, 4, and 6 h postdose.

[h]Five samples: samples at 2, 3, 4, 5, and 6 h postdose.

Abbreviations: AUC, area under the concentration-time curve; LLOA, lower limit of agreement; ULOA, upper limit of agreement; RMSPE%, percentage root mean squared prediction error.

studies.[24,44,45] Our results showed that BSA had a significant effect on Vd and CL ($p < 0.001$), which is consistent with previous studies.[24,44,45] For a typical patient with a BSA of 1.69 m^2, the population estimates of CL and Vd were 8.24 L·h^{-1} and 29.70 L, respectively. This result is in good accordance with the study of Takama et al.[44] (CL = 8.87 L·h^{-1} and Vd = 33.80 L). In the Choe et al.[22] study, which included only adult patients with i.v. BU, the IIV for CL and Vd were 16% and 9%, respectively. However, the corresponding values in children were reported as 23% and 11% by Booth et al.,[46] which suggested that greater IIV in BU PK parameters was observed in children compared to adults. In the present study, the IIV of CL and Vd were 22.00% and 13.60%, respectively, which was comparable to the values from Wu et al.[47] (IIV of CL and Vd were 18.40% and 18.70%). The possible reason for the increased IIV compared with the study of Choe et al.[22] might be associated with the mixed population enrolled (adults and children) in the current study.

Our results showed that ALP significantly affected Vd ($p < 0.001$), with a negative correlation between them. BU is extensively metabolized by the liver through the glutathione conjugation pathway, and alteration of liver function may affect the elimination of BU.[48,49] ALP is an indicator of liver function. The decrease of ALP might affect the synthesis of albumin, resulting in the increased free BU in plasma and eventually elevating the Vd.[50] The majority of the enrolled patients ($n = 54$, 81.8%) were greater than or equal to 18 years old, and 12 were children (range: 6–17 years old). McCune et al.[51] showed that BU CL is predicted to be 95% of the adult clearance at 2.5 years of age, and the CL of patients more than 2.5 years old did not change with age. It is reasonable that we did not find that age had a significant effect on BU PKs, which is similar to some reported studies.[44,47] Anti-fungal treatment is commonly used in patients with HSCT. Voriconazole is an enzyme inhibitor that can affect the activity of CYP2C9, CYP2C19, and CYP3A4.[52] Phenytoin sodium is used to prevent epilepsy caused by high-dose BU, which is a strong liver enzyme inducer of CYP3A4.[53] The activity of GST has not been documented to be influenced by them, it is reasonable that no drug interaction exists between BU and these two medications. Fludarabine combined with BU is used as the conditioning regimen prior to HSCT, which is dephosphorylated to F-ara-A by 5′-nucleotidase.[54] Its impact on BU metabolism remains controversial.[54–57] Cyclosporin A is an essential drug for graft versus host disease prophylaxis in HSCT, which is metabolized by CYP3A4 and CYP3A5.[58] Due to the different metabolic pathways, it is reasonable that their effects on BU PKs were not observed in the current study. Anti-emetics may affect the disposition of oral BU by increasing its absorption and bioavailability, but they do not play a major role in the course of i.v. BU disposition.[47] Other PopPK models included covariates, such as SEX, ALT, GSTA1,[21,22,45] but none affected CL and Vd in our study. The saliva model was not significantly improved by including other covariates. The residual error of plasma was lower than the saliva (12.92% vs. 22.50%), indicating a higher degree of unexplained variability in the saliva concentration.

The AUC$_{ss}$ within each dose interval is equal to the AUC$_{0-\infty}$ after dose one. Takama et al.[44] has shown that the interoccasion variability (IOV) in CL was only 6.6%, which was less than the intra-individual variability. Therefore,

the prediction performance of AUC_{ss} was verified by calculating the $AUC_{0-\infty}$ after dose one. Plasma and salivary concentrations at different times after the first dose were simulated in 3000 fictional patients. Bayesian MAP optimization and linear regression were used to assess the predictive performance of the saliva PopPK model. There are several advantages to using Bayesian methodology.[31] First, Bayesian methodology might result in a lower RMSPE% and a narrower LOA range than linear regression, indicating its superior predictability to the latter. Additionally, Bayesian methodology takes residual variation into account. Therefore, the extrapolation from outlier saliva observations to extreme predicted AUC_{ss} was prevented. Third, in contrast to the method of linear regression, the estimates of Bayesian MAP optimization cannot exceed the constraints provided by the population model. Finally, the information obtained from multiple samples can be used to estimate the most likely AUC_{ss}, thus reducing the prediction error. It indicated that the predictive performance of the PopPK model might be improved with the increase of saliva samples. The simulation confirmed that saliva sampling was eminently feasible for the estimation of individual AUC_{ss} in the clinical practice.

Based on the final PopPK model, the calculator tool for the initial dose was designed for individualized BU therapy in clinical practice. The equation for the initial dose of BU in units of milligrams is:

$$CL_i \ (L/h) = 8.24 \times \left(\frac{BSA_i}{1.69} \right)^{0.99} \tag{5}$$

$$Dose \ (mg) = AUC_{target} \times CL_i \tag{6}$$

After dosing, one sample concentration is sufficient for the latter dose adjustment. Although other timepoint sample is also feasible, we recommend measuring the BU salivary trough concentration (6h after the first dose) due to its convenience to obtain. The individual CL and AUC are estimated using Bayesian estimation method based on the salivary trough concentration. If AUC is not within the target treatment range, the dose is adjusted with CL obtained from the Bayesian method.

There are several limitations in the present study. First, we did not consider the mechanism by which the drug in saliva could be re-absorbed when it is swallowed. The bio-availability can reach 70%–90% when BU is administered orally, which may extend the duration of drug action in vivo and increase the BU concentration. The re-absorption of drug in saliva may result in double peaks, like hepato-enteral circulation. However, we did not observe another peak in the elimination phase, which indicate that re-absorption has limited effect on the characteristic of the PK

profile of i.v. BU (Figure S7). In addition, the PopPK model for plasma and saliva was developed using concentrations after the first dose of BU, which was not allowed to estimate the IOV. Several reports[44,45,59] considered the IOV in CL and Vd, indicating the change of PK parameters over time. However, considering the limited dosing time of BU (a totally 3 or 4days), ignoring IOV may not lead to a significant bias of the estimated PK parameters or a falsely optimistic impression of the potential use of salivary BU concentration in model-informed precision dosing.[60] Finally, covariates or IIV for the saliva drug penetration were not modeled by a scale-factor in our study. The shrinkage value of the scale-factor IIV reached 100%, suggesting that the individual information obtained may be insufficient to estimate the IIV for each parameter in the model. It can be solved by obtaining more samples from each patient in future studies.

CONCLUSIONS

The developed PopPK model adequately describes the saliva and plasma PK of i.v. BU in Chinese patients undergoing HSCT. Internal validation of the final model demonstrated its robustness. Meanwhile, the simulation results indicate that AUC_{ss} can be predicted from saliva concentration by Bayesian MAP optimization. This study provides a methodology for developing saliva and plasma models for other drugs to promote the popularization and application of noninvasive salivary sampling in model-informed precision dosing.

AUTHOR CONTRIBUTIONS

B.X. and T.Y. wrote the manuscript. X.W. and M.L. designed the research. B.X., Q.L., and D.L. performed the research. J.Z., Y.Z., Y.Z., and J.W. analyzed the data.

CONFLICT OF INTEREST STATEMENT

The authors declared no competing interests for this work.

ORCID

Jianxing Zhou https://orcid.org/0000-0003-4405-0440
Qingxia Liu https://orcid.org/0000-0002-4100-5735
Xuemei Wu https://orcid.org/0000-0003-1640-7385

REFERENCES

1. Fisher VL, Barnes YJ, Nuss SL. Pretransplant conditioning in adults and children: dose assurance with intravenous busulfan. *Oncol Nurs Forum*. 2006;33:E36-E43.

2. Speziali C, Daly A, Abuhaleeqa M, et al. Fludarabine, busulfan, and low-dose TBI conditioning versus cyclophosphamide and TBI in allogeneic hematopoietic cell transplantation for adult acute lymphoblastic leukemia. *Leuk Lymphoma*. 2019;60:639-648.

3. ten Brink MH, Zwaveling J, Swen JJ, Bredius RGM, Lankester AC, Guchelaar HJ. Personalized busulfan and treosulfan conditioning for pediatric stem cell transplantation: the role of pharmacogenetics and pharmacokinetics. *Drug Discov Today*. 2014;19:1572-1586.

4. Copelan EA, Hamilton BK, Avalos B, et al. Better leukemia-free and overall survival in AML in first remission following cyclophosphamide in combination with busulfan compared with TBI. *Blood*. 2013;122:3863-3870.

5. Lee JH, Choi SJ, Lee JH, et al. Decreased incidence of hepatic veno-occlusive disease and fewer hemostatic derangements associated with intravenous busulfan vs oral busulfan in adults conditioned with busulfan + cyclophosphamide for allogeneic bone marrow transplantation. *Ann Hematol*. 2005;84:321-330.

6. Grochow LB, Jones RJ, Brundrett RB, et al. Pharmacokinetics of busulfan: correlation with veno-occlusive disease in patients undergoing bone marrow transplantation. *Cancer Chemother Pharmacol*. 1989;25:55-61.

7. Vassal G. Pharmacologically-guided dose adjustment of busulfan in high-dose chemotherapy regimens: rationale and pitfalls (review). *Anticancer Res*. 1994;14:2363-2370.

8. Andersson BS, Madden T, Tran HT, et al. Acute safety and pharmacokinetics of intravenous busulfan when used with oral busulfan and cyclophosphamide as pretransplantation conditioning therapy: a phase I study. *Biol Blood Marrow Transplant*. 2000;6:548-554.

9. Rhee SJ, Lee JW, Yu KS, et al. Pediatric patients undergoing hematopoietic stem cell transplantation can greatly benefit from a novel once-daily intravenous busulfan dosing nomogram. *Am J Hematol*. 2017;92:607-613.

10. Anderson BJ, McKee AD, Holford NH. Size, myths and the clinical pharmacokinetics of analgesia in paediatric patients. *Clin Pharmacokinet*. 1997;33:313-327.

11. Ehrsson H, Hassan M, Ehrnebo M, Beran M. Busulfan kinetics. *Clin Pharmacol Ther*. 1983;34:86-89.

12. Palmer J, McCune JS, Perales MA, et al. Personalizing busulfan-based conditioning: considerations from the American Society for Blood and Marrow Transplantation Practice Guidelines Committee. *Biol Blood Marrow Transplant*. 2016;22:1915-1925.

13. Nguyen L, Fuller D, Lennon S, Leger F, Puozzo C. I.V. busulfan in pediatrics: a novel dosing to improve safety/efficacy for hematopoietic progenitor cell transplantation recipients. *Bone Marrow Transplant*. 2004;33:979-987.

14. Slattery JT, Clift RA, Buckner CD, et al. Marrow transplantation for chronic myeloid leukemia: the influence of plasma busulfan levels on the outcome of transplantation. *Blood*. 1997;89:3055-3060.

15. Dix SP, Wingard JR, Mullins RE, et al. Association of busulfan area under the curve with veno-occlusive disease following BMT. *Bone Marrow Transplant*. 1996;17:225-230.

16. Tang W, Wang L, Zhao WL, Chen YB, Shen ZX, Hu J. Intravenous busulfan-cyclophosphamide as a preparative regimen before allogeneic hematopoietic stem cell transplantation for adult patients with acute lymphoblastic leukemia. *Biol Blood Marrow Transplant*. 2011;17:1555-1561.

17. Widness JA. Pathophysiology of anemia during the neonatal period, including anemia of prematurity. *Neoreviews*. 2008;9:e520.

18. Gröschl M, Rauh M, Dörr HG. Circadian rhythm of salivary cortisol, 17alpha-hydroxyprogesterone, and progesterone in healthy children. *Clin Chem*. 2003;49:1688-1691.

19. Hutchinson L, Sinclair M, Reid B, Burnett K, Callan B. A descriptive systematic review of salivary therapeutic drug monitoring in neonates and infants. *Br J Clin Pharmacol*. 2018;84:1089-1108.

20. Rauh M, Stachel D, Kuhlen M, Gröschl M, Holter W, Rascher W. Quantification of busulfan in saliva and plasma in haematopoietic stem cell transplantation in children: validation of liquid chromatography tandem mass spectrometry method. *Clin Pharmacokinet*. 2006;45:305-316.

21. Choi B, Kim MG, Han N, et al. Population pharmacokinetics and pharmacodynamics of busulfan with GSTA1 polymorphisms in patients undergoing allogeneic hematopoietic stem cell transplantation. *Pharmacogenomics*. 2015;16:1585-1594.

22. Choe S, Kim G, Lim HS, et al. A simple dosing scheme for intravenous busulfan based on retrospective population pharmacokinetic analysis in korean patients. *Korean J Physiol Pharmacol*. 2012;16:273-280.

23. Sun Y, Huang J, Hao C, et al. Population pharmacokinetic analysis of intravenous busulfan: GSTA1 genotype is not a predictive factor of initial dose in Chinese adult patients undergoing hematopoietic stem cell transplantation. *Cancer Chemother Pharmacol*. 2020;85:293-308.

24. Nguyen L, Leger F, Lennon S, Puozzo C. Intravenous busulfan in adults prior to haematopoietic stem cell transplantation: a population pharmacokinetic study. *Cancer Chemother Pharmacol*. 2006;57:191-198.

25. Xie HZB, Wu X, Zou C, Huang X, Huang X, Lou Y. Determination of busulfan plasma drug concentration by HPLC-MS/MS. *Strait Pharmaceut J*. 2014;26:243-246.

26. Paci A, Vassal G, Moshous D, et al. Pharmacokinetic behavior and appraisal of intravenous busulfan dosing in infants and older children: the results of a population pharmacokinetic study from a large pediatric cohort undergoing hematopoietic stem-cell transplantation. *Ther Drug Monit*. 2012;34:198-208.

27. Wicha SG, Mundkowski RG, Klock A, et al. Is moxifloxacin a treatment option for pancreatic infections? A Pharmacometric analysis of serum and pancreatic juice. *J Clin Pharmacol*. 2019;59:1405-1414.

28. Bergstrand M, Hooker AC, Wallin JE, Karlsson MO. Prediction-corrected visual predictive checks for diagnosing nonlinear mixed-effects models. *AAPS J*. 2011;13:143-151.

29. Kruizinga MD, Stuurman FE, Driessen GJA, Cohen AF, Bergmann KR, van Esdonk MJ. Theoretical performance of nonlinear mixed-effect models incorporating saliva as an alternative sampling matrix for therapeutic drug monitoring in pediatrics: a simulation study. *Ther Drug Monit*. 2021;43:546-554.

30. Kang D, Bae KS, Houk BE, Savic RM, Karlsson MO. Standard error of empirical Bayes estimate in NONMEM® VI. *Korean J Physiol Pharmacol*. 2012;16:97-106.

31. Kruizinga MD, Zuiker RGJA, Bergmann KR, et al. Population pharmacokinetics of clonazepam in saliva and plasma: steps towards noninvasive pharmacokinetic studies in vulnerable populations. *Br J Clin Pharmacol*. 2022;88:2236-2245.

32. Taraji M, Haddad PR, Amos RIJ, et al. Error measures in quantitative structure-retention relationships studies. *J Chromatogr A*. 2017;1524:298-302.

33. Giavarina D. Understanding Bland Altman analysis. *Biochem Med (Zagreb)*. 2015;25:141-151.

34. Beal SL. Ways to fit a PK model with some data below the quantification limit. *J Pharmacokinet Pharmacodyn*. 2001;28:481-504.

35. Bezinelli LM, Eduardo FP, de Carvalho DLC, et al. Therapeutic salivary monitoring of IV busulfan in patients undergoing hematopoietic stem cell transplantation: a pilot study. *Bone Marrow Transplant*. 2017;52:1384-1389.

36. de Paula EF, Bezinelli LM, Carvalho DLC, et al. Is salivary busulfan the cause of Oral mucositis and the changes in salivary antioxidant enzymes after hematopoietic cell transplantation? *Ther Drug Monit*. 2020;42:565-571.

37. Russell JA, Kangarloo SB. Therapeutic drug monitoring of busulfan in transplantation. *Curr Pharm des*. 2008;14:1936-1949.

38. Haeckel R. Factors influencing the saliva/plasma ratio of drugs. *Ann N Y Acad Sci*. 1993;694:128-142.

39. Mathew RJ, Weinman M, Claghorn JL. Xerostomia and sialorrhea in depression. *Am J Psychiatry*. 1979;136:1476-1477.

40. Gordi T, Hai TN, Hoai NM, Thyberg M, Ashton M. Use of saliva and capillary blood samples as substitutes for venous blood sampling in pharmacokinetic investigations of artemisinin. *Eur J Clin Pharmacol*. 2000;56:561-566.

41. Huffman DH. Relationship between digoxin concentrations in serum and saliva. *Clin Pharmacol Ther*. 1975;17:310-312.

42. Tsiropoulos I, Kristensen O, Klitgaard NA. Saliva and serum concentration of lamotrigine in patients with epilepsy. *Ther Drug Monit*. 2000;22:517-521.

43. McAuliffe JJ, Sherwin AL, Leppik IE, Fayle SA, Pippenger CE. Salivary levels of anticonvulsants: a practical approach to drug monitoring. *Neurology*. 1977;27:409-413.

44. Takama H, Tanaka H, Nakashima D, Ueda R, Takaue Y. Population pharmacokinetics of intravenous busulfan in patients undergoing hematopoietic stem cell transplantation. *Bone Marrow Transplant*. 2006;37:345-351.

45. Sandström M, Karlsson MO, Ljungman P, et al. Population pharmacokinetic analysis resulting in a tool for dose individualization of busulphan in bone marrow transplantation recipients. *Bone Marrow Transplant*. 2001;28:657-664.

46. Booth BP, Rahman A, Dagher R, et al. Population pharmacokinetic-based dosing of intravenous busulfan in pediatric patients. *J Clin Pharmacol*. 2007;47:101-111.

47. Wu X, Xie H, Lin W, et al. Population pharmacokinetics analysis of intravenous busulfan in Chinese patients undergoing hematopoietic stem cell transplantation. *Clin Exp Pharmacol Physiol*. 2017;44:529-538.

48. Gibbs JP, Liacouras CA, Baldassano RN, Slattery JT. Upregulation of glutathione S-transferase activity in enterocytes of young children. *Drug Metab Dispos*. 1999;27:1466-1469.

49. Czerwinski M, Gibbs JP, Slattery JT. Busulfan conjugation by glutathione S-transferases alpha, mu, and pi. *Drug Metab Dispos*. 1996;24:1015-1019.

50. Shimoda M, Kokue E, Hayama T, Vree TB. Effect of albumin distribution. A simulation analysis of the effect of altered albumin distribution on the apparent volume of distribution and apparent elimination rate constant of drugs. *Pharm Weekbl Sci*. 1989;11:87-91.

51. McCune JS, Bemer MJ, Barrett JS, Scott Baker K, Gamis AS, Holford NH. Busulfan in infant to adult hematopoietic cell transplant recipients: a population pharmacokinetic model for initial and Bayesian dose personalization. *Clin Cancer Res*. 2014;20:754-763.

52. Niwa T, Shiraga T, Takagi A. Effect of antifungal drugs on cytochrome P450 (CYP) 2C9, CYP2C19, and CYP3A4 activities in human liver microsomes. *Biol Pharm Bull*. 2005;28:1805-1808.

53. Beumer JH, Owzar K, Lewis LD, et al. Effect of age on the pharmacokinetics of busulfan in patients undergoing hematopoietic cell transplantation; an alliance study (CALGB 10503, 19808, and 100103). *Cancer Chemother Pharmacol*. 2014;74:927-938.

54. de Castro FA, Lanchote VL, Voltarelli JC, Colturato VA, Simões BP. Influence of fludarabine on the pharmacokinetics of oral busulfan during pretransplant conditioning for hematopoietic stem cell transplantation. *J Clin Pharmacol*. 2013;53:1205-1211.

55. Yeh RF, Pawlikowski MA, Blough DK, et al. Accurate targeting of daily intravenous busulfan with 8-hour blood sampling in hospitalized adult hematopoietic cell transplant recipients. *Biol Blood Marrow Transplant*. 2012;18:265-272.

56. Almog S, Kurnik D, Shimoni A, et al. Linearity and stability of intravenous busulfan pharmacokinetics and the role of glutathione in busulfan elimination. *Biol Blood Marrow Transplant*. 2011;17:117-123.

57. de Lima M, Couriel D, Thall PF, et al. Once-daily intravenous busulfan and fludarabine: clinical and pharmacokinetic results of a myeloablative, reduced-toxicity conditioning regimen for allogeneic stem cell transplantation in AML and MDS. *Blood*. 2004;104:857-864.

58. Cvetković M, Zivković M, Bundalo M, et al. Effect of age and allele variants of CYP3A5, CYP3A4, and POR genes on the pharmacokinetics of cyclosporin a in pediatric renal transplant recipients from Serbia. *Ther Drug Monit*. 2017;39:589-595.

59. Schiltmeyer B, Klingebiel T, Schwab M, et al. Population pharmacokinetics of oral busulfan in children. *Cancer Chemother Pharmacol*. 2003;52:209-216.

60. Karlsson MO, Sheiner LB. The importance of modeling interoccasion variability in population pharmacokinetic analyses. *J Pharmacokinet Biopharm*. 1993;21:735-750.

SUPPORTING INFORMATION

Additional supporting information can be found online in the Supporting Information section at the end of this article.